THE JOURNAL OF PHYSICAL CHEMISTRY C

Article

Cite This: J. Phys. Chem. C XXXX, XXX, XXX−XXX

pubs.acs.org/JPCC

First-Principles Approach to the Conductance of Covalently Bound Molecular Junctions

Published as part of The Journal of Physical Chemistry virtual special issue "Abraham Nitzan Festschrift".

Sivan Refaely-Abramson,[†,‡] Zhen-Fei Liu,[†,‡] Fabien Bruneval,[§] and Jeffrey B. Neaton*[,†,‡,∥]

[†]Molecular Foundry, Lawrence Berkeley National Laboratory, Berkeley, California 94720, United States

[‡]Department of Physics, University of California Berkeley, Berkeley, California 94720, United States

[§]DEN, Service de Recherches de Métallurgie Physique, CEA, Université Paris-Saclay, F-91191 Gif-sur-Yvette, France

[∥]Kavli Energy Nanosciences Institute at Berkeley, Berkeley, California 94720, United States

Supporting Information

ABSTRACT: We develop a first-principles approach for accurate conductance calculations of covalently bound molecular junctions. Our approach extends the DFT+Σ method, an approximate *GW*-based self-energy correction scheme acting on a tractable molecular subspace (based on a gas-phase reference of the same dimension) that corrects level alignment in the junction relative to density functional theory (DFT). We introduce a new extended gas-phase reference system, consisting of the molecule and several lead atoms, whose frontier orbitals maximally project onto the conducting orbitals of the junction. With this choice of reference, our self-energy correction to the Kohn−Sham Hamiltonian takes into account mixing of the gas-phase reference orbitals upon the formation of the junction. We apply our generalized DFT+Σ approach to a series of alkane−chain junctions in which the molecules are covalently bound to the leads via carboxyl terminal groups. Our results lead to conductance values in quantitative agreement with experiment. We also revisit the well-studied Au−bipyridine−Au junction and show that we recover the original DFT+Σ approach for relatively weak donor−acceptor molecule−lead binding.

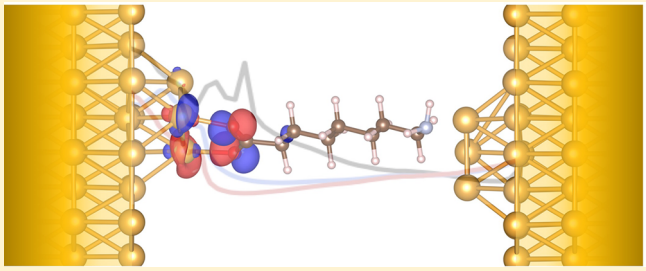

INTRODUCTION

Molecular junctions, individual molecules connected to macroscopic electrodes, are a unique means of probing charge-transport processes on the nanoscale.[1,2] Extensive prior research on such junctions includes both experimental[2−7] and theoretical[1,8−10] work. Experimental approaches allow the measurement of individual molecules in junctions under a variety of nonequilibrium conditions,[11−13] in a variety of environments,[14,15] and with a variety of electrode−molecule interfacial bonding chemistries.[16−19] Because there is no means yet of visualizing junction structure on the atomic scale in operando, accurate ab initio calculations are essential in interpreting and driving experiments, associating chemical structures with junction functionality. This requires sophisticated theoretical approaches,[20,21] capable of handling complex structures while predicting tunneling properties quantitatively as a function of bias,[22−25] for different manners of molecule−electrode bridging,[26−29] in different solvent environments,[30−32] under dynamical conditions where reactions may occur,[33,34] and even while optically or thermally driven.[35,36]

Theoretical calculations of charge transport through molecular junctions are typically performed within the nonequilibrium Green's function (NEGF) formalism,[37,38] employing density functional theory (DFT) for the electronic structure.[39−41] It is well known, however, that standard local and semilocal Kohn−Sham (KS) DFT approaches underestimate the fundamental gap of the molecule[42−46] and do not lead to reliable level alignment between molecular frontier orbital energies and the Fermi level (E_F) of the junction.[47,48] As a result, the calculated zero-bias conductances are typically too high compared with experimental measurements.[49] One way to overcome this deficiency is to introduce many-body corrections to KS eigenvalues within the *GW* approximation[50−52] (where *G* stands for Green's function and *W* stands for the screened Coulomb interaction), in which nonlocal correlation effects are captured.[53] Prior work[47] established that *GW* can be used to accurately capture such effects and that such effects are large. However, *GW* approaches have significant limitations: Computing junctions consisting of molecules of chemical and biological interest can be of enormous computational expense. In addition, the *GW* results strongly depend on the DFT starting point,[54,55] and often the involved wave functions and energies need to be iterated to self-consistency to reach the required accuracy.[54,56] These

Received: December 17, 2018
Revised: February 13, 2019
Published: February 22, 2019

J. Phys. Chem. C
Downloaded from pubs.acs.org by EAST CAROLINA UNIV on 03/08/19. For personal use only.

 © XXXX American Chemical Society

DOI: 10.1021/acs.jpcc.8b12124
J. Phys. Chem. C XXXX, XXX, XXX−XXX

limitations prohibit, in this stage, routine *GW* calculations of molecular junctions, and alternative theoretical approaches that improve the DFT energy levels have been suggested.[53,57−59]

A successful approach to reduce the computational cost while maintaining the accuracy is the DFT+Σ method, first introduced in ref 49. In this framework, the molecular energy levels are corrected via a *GW*-like self-energy, which is partitioned into two terms in a tractable molecular subspace: one that corrects the molecular gas-phase KS orbital energies to their spectroscopic values and one that incorporates nonlocal polarization effects due to the metal electrode.[47,49] The computational cost of DFT+Σ is greatly reduced relative to a full *GW* calculation, as the subsystem on which the full *GW* self-energy is evaluated is relatively small. DFT+Σ has been highly successful in the weak-coupling limit, a limit where the molecule's frontier orbitals are minimally perturbed by the junction, and was shown to reproduce experimental results for many molecular junctions.[60−63] However, this scheme is expected to break down in covalently bound junctions, as we detail below. Because many systems of interest do involve covalent bonds between the molecule and the leads[64,65] and because full *GW* calculations on junctions continue to be far from routine, it is important to seek generalizations of the original DFT+Σ framework, in which quasiparticle self-energy corrections are applied in a tractable subspace of the junction, to properly account for such strongly bound junctions as well.

In this work, we develop a generalization of the DFT+Σ framework to treat covalently bound molecular junctions. We propose a new definition of the gas-phase reference system and the gas-phase correction term in the approximate Σ used in this approach. To better account for the hybridization between the molecule and the leads, we expand the junction orbitals in the basis of gas-phase orbitals of a reference system that includes some lead atoms. We apply our new scheme to a series of covalently bound alkane-chain junctions and more weakly bound Au−bipyridine (BP)−Au junctions and show that our new approach leads to quantitative agreement with experiment.

■ METHODS

Within the NEGF framework, the junction system is partitioned into three regions: the left (L) and right (R) leads and the contact region (C) that contains the molecule and a few layers of lead atoms. Figure 1 shows the two representative molecular junctions we use to demonstrate our new approach: a seven-carbon alkane chain molecule (a) and a BP molecule (b) in contact with Au leads. In both cases, the C region contains the molecule, a gold trimer linker group, and four layers of gold atoms on each side. As implemented in the TranSIESTA package,[40] the Hamiltonians of L and R regions are obtained via DFT calculations of the bulk leads, whereas the Hamiltonian of the C region is calculated self-consistently with open boundary conditions. The junction conductance is then evaluated with the Landauer formula,[38] which requires the Green's function of the contact region

$$G(E) = [E - H - \Sigma_L(E) - \Sigma_R(E)]^{-1} \quad (1)$$

where H is the Hamiltonian of the contact region and $\Sigma_{L/R}(E)$ is the self-energy representing the effect of the semi-infinite left/right electrode, respectively.

In DFT+Σ, we introduce a separate self-energy Σ in the subspace of the central region Hamiltonian H to correct the KS

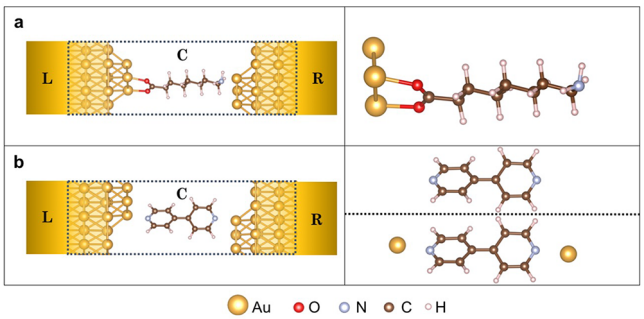

Figure 1. Representative molecular junctions studied in this work: (a) $NH_2(CH_2)_7COOH$, where the alkane chain binds to Au trimers via peptide-like carboxyl terminal groups, and (b) bipyridine, where the nitrogen binds to Au trimers via donor−acceptor bonds. L and R regions represent the semi-infinite electrodes, and C is the contact region. The reference systems used in the DFT+Σ calculations are shown to the right of each junction.

eigenvalues for missing exchange and correlation effects (the Σ in DFT+Σ). While prior work has performed a more rigorous *GW* calculation on molecular junctions to evaluate Σ,[58,66,67] such an approach is not yet feasible for many increasingly complex systems of interest. Instead, here we work within the DFT+Σ framework described above, generalizing it to covalently bound junctions. The idea behind DFT+Σ is to employ a molecular reference, a tractable subsystem of the junction whose electronic structure is mainly responsible for the transport properties, and define self-energy corrections of the orbital eigenvalues of the reference upon its connection to electrodes in a junction. Note that the self-energy of interest in this work is due to many-body effects that are missing in local and semilocal DFT calculations, not the tunneling self-energy due to one-body electronic coupling between the molecule and the electrodes, which in many cases of interest is already captured by local and semilocal functionals.[68] As mentioned, the DFT+Σ framework is a *GW*-inspired model correction that involves two parts: First, a gas-phase term corrects DFT eigenvalues to electron addition and removal quasiparticle energies, which can be calculated using a variety of methods, such as via total energy differences (i.e., the so-called ΔSCF method), predictive hybrid functional approaches as in ref 63, or within *GW*; a second correction term accounts for nonlocal surface polarization, which is often approximated, for example, via a classical electrostatic image-charge model[47] requiring the definition of an image plane.[69] We note that the DFT+Σ approach is not a simple empirical scissors shift; no empirical parameters are used, and Σ is calculated from first-principles for each system. In addition, the DFT+Σ correction is, in principle, orbital-dependent.

In the original DFT+Σ framework,[49,60] we write the self-energy δH of the central region as

$$\delta H = \sum_{\mu} \Sigma_{\mu} |\psi_{\mu}^{gp}\rangle\langle\psi_{\mu}^{gp}| \quad (2)$$

In eq 2, $|\psi^{gp}\rangle$ is a gas-phase reference KS orbital, and μ is its index. μ runs over occupied and unoccupied states in principle. Σ_{μ} is an orbital-dependent energy correction term for each gas-phase state μ. In previous works, the reference system was defined simply as the molecule in the junction. The self-energy is then defined and evaluated only in the reference subblock of the Hamiltonian, whose dimension is defined as a smaller

DOI: 10.1021/acs.jpcc.8b12124
J. Phys. Chem. C XXXX, XXX, XXX−XXX

subspace associated with the molecule, as shown in eq 2. To distinguish the reference orbitals of the isolated molecule and those in the junction, we denote the gas-phase orbitals of the reference system by $\{\psi_i^{gp}\}$ and the eigenvectors of the subblock of the junction KS Hamiltonian corresponding to the reference subspace by $\{\phi_i\}$, and we call ϕ_i the junction orbital. In the basis of junction orbitals, δH has the form

$$\langle\phi_i|\delta H|\phi_j\rangle = \sum_\mu \Sigma_\mu \langle\phi_i|\psi_\mu^{gp}\rangle\langle\psi_\mu^{gp}|\phi_j\rangle \tag{3}$$

One can transform between the two basis sets via a unitary transformation. We note in passing that for simplicity all equations used in this work assume an orthonormal basis set. With a nonorthogonal basis set that is used in, for example, SIESTA,[70] the equations need to be modified accordingly to reflect the overlap matrix. We also note that the limit eq 3 represents neglects frequency-dependent screening effects and strong correlations that give rise to, for example, the Kondo effect; eq 3 also relies on the assumption that the KS wave functions are a good approximation of the true quasiparticle states.

In the case of weakly bound junctions, for which DFT+Σ was originally developed, the junction orbitals and gas-phase reference orbitals are very similar, at least for the frontier states that dominate the charge transport. More precisely, for each gas-phase molecular orbital ψ_μ^{gp} of relevance for transmission, there exists a junction orbital ϕ_i whose overlap is close to unity, that is

$$\langle\phi_i|\psi_\mu^{gp}\rangle \approx 1 \tag{4}$$

As a result, the left-hand side of eq 3 becomes diagonal in the basis of junction orbitals given the orthonormalization condition of $\{\phi_i\}$. Introducing the diagonal terms, we have[47,49]

$$\delta H_{ii} = \langle\phi_i|\delta H|\phi_i\rangle := \Sigma_i = \Delta_i + P_i \tag{5}$$

where Δ_i and P_i are gas-phase and nonlocal polarization corrections for the molecular orbital i. Usually Δ_i is negative (positive) for an occupied (unoccupied) molecular orbital and P_i is positive (negative) for an occupied (unoccupied) molecular orbital. The partitioning of δH_{ii} into the above two contributions becomes exact if there is only one junction orbital ϕ_i sufficiently far from E_F, whose inner product with ψ_i^{gp} is unity. The Δ_i term in eq 5 can be calculated rather accurately and efficiently. Whereas in previous studies ΔSCF was used,[49] as well as advanced hybrid functionals,[63] to correct the molecular KS energy levels, here we use both a one-shot G_0W_0 calculation and an optimally tuned range-separated hybrid (OT-RSH) functional[46] (see the Supporting Information (SI)).

Physically, the original DFT+Σ framework is suitable for junctions in which the hybridization and electronic coupling between the molecule and the electrodes are relatively weak, resulting in Lorentzian-like lineshapes[71] for the transmission function, $T(E)$. In this weak-coupling limit, the gas-phase molecule serves as a natural "reference", whose orbital resembles the conductance eigenchannel. However, for strongly bound junctions, the covalent binding does not lead to Lorentzian lineshapes, the assumption of a near-unity projection breaks down, and the weak-coupling limit of DFT+Σ is not well satisfied. This is because, in such cases, a chemical bond is usually broken when the junction forms, which leads to strong hybridization of molecular orbitals with lead states. The identification of a gas-phase reference system becomes nontrivial because the orbitals of the junction molecule in its closed-shell form may not resemble the conducting orbitals of the molecule when in the junction. Below, we address this issue by defining extended reference gas-phase systems that include hybridization between molecular orbitals and lead states in covalently bound junctions.

The rest of this Article is organized as follows. We first examine a series of molecular junctions composed of short linear alkane chains, $NH_2(CH_2)_nCOOH$, covalently bound to Au leads, as shown schematically in Figure 1a. This system was recently examined experimentally.[64] The strong hybridization in the junction challenges the applicability of the original DFT+Σ framework to predict and explain experimental observations, but with the new choice of gas-phase reference system proposed here, we overcome these challenges. We then revisit the well-studied Au−BP−Au junction (Figure 1b), where the molecule is linked to the leads via weakly coupled donor−acceptor bonds. We explore two different possible choices for the reference system in this well-studied junction and show that in the limit of weak coupling, the bare gas-phase molecule is a more suitable reference and our new approach reduces to the original form of DFT+Σ.

Our DFT transmission calculations use the Perdew−Burke−Ernzerhof (PBE) functional.[72] We use SIESTA[70] for the geometry optimization and the electronic structure calculations of the junction and TranSIESTA[40] for transport calculations. DFT calculations of the energy levels and orbitals of gas-phase reference systems studied here are performed using the Q-Chem package,[73] and *GW* calculations of the gas-phase systems are performed using the MOLGW package.[74] (See the SI for full computational details.)

■ RESULTS AND DISCUSSION

We begin by demonstrating our method on molecular junctions consisting of short alkane chains bound to Au leads. Molecular junctions of alkane chains with donor−acceptor linkers are well studied in both experiment[75−79] and theory,[79−81] including within the DFT+Σ framework.[61] Here, however, we consider chains terminated with more strongly bound peptide-like groups of −COOH, mimicking binding motifs of biological molecular systems. When connected to Au leads in the junction, the H atom is removed and covalent O−Au bonds are formed.[82] The conductance of these junctions was recently measured using a scanning-tunneling-microscope-based break-junction method.[64]

A representative example of a junction studied here, containing an alkane chain with seven carbon atoms (C7), is shown schematically in Figure 1a. Importantly, the molecule alone, $NH_2-(CH_2)_n-COO^-$, is no longer a good gas-phase reference system for DFT+Σ, as originally formulated: It is not a closed-shell system, as the COO− group is missing a H atom, and the transmission is dominated by strongly hybridized molecule−lead states due to the covalent binding between them. Applying a standard gas-phase shift (Δ_i in eq 5) corresponding to a bare gas-phase molecular orbital $|\psi_i^{gp}\rangle$ requires cutting a bond in the reference calculation and is hence inappropriate. Instead, we use an extended system as the gas-phase reference that includes a few Au atoms from the leads that participate in the hybridization and binding. Below, we explain how we choose this new reference system and present a generalized form of Σ to account for the gas-phase correction involved.

DOI: 10.1021/acs.jpcc.8b12124
J. Phys. Chem. C XXXX, XXX, XXX−XXX

We start by computing the DFT-PBE transmission curve of the strongly bound C7 junction (black line in Figure 2 (top)).

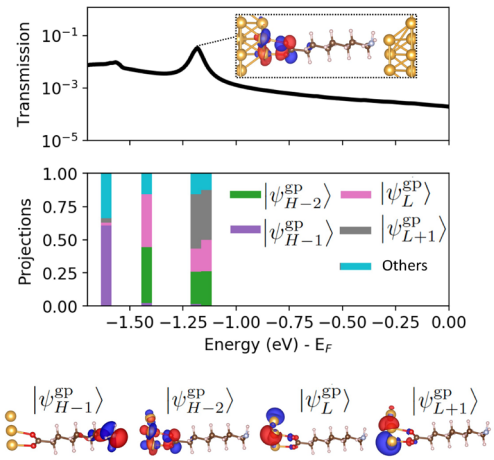

Figure 2. Top: DFT-PBE transmission as a function of energy relative to E_F for the C7 molecular junction. Inset: the eigenchannel associated with the HOMO resonant peak. Bottom: projection coefficients $|C|^2$ of the resonance state and other unoccupied levels around E_F for the C7+Au$_3$ reference system discussed in the text. Each color represents a different gas-phase orbital, as shown in the figure.

A resonance peak in the transmission curve appears around 1.2 eV below E_F. The calculated charge distribution associated with this channel (or eigenchannel[83]) is shown in Figure 2 (inset). Importantly, this eigenchannel is mainly localized on the carboxylic terminal group and the Au trimer bound to it. This suggests that the zero bias conductance of this junction originates from hybridized states localized on covalent O−Au bonds. Thus, in considering corrections to the DFT conductance, it is insufficient to account for the organic part of the junction alone, and we consider an extended reference containing the Au atoms participating in the strong binding. However, to use such a reference system to construct the gas-phase correction (Δ_i in eq 5), we can no longer assume that eq 4 holds, namely, that the gas-phase orbitals of the reference system project cleanly onto the molecular states in the junction.

To address this issue, we generalize the DFT+Σ approach and expand the junction molecular states $|\phi_i\rangle$ in the basis of states $|\psi_\mu^{gp}\rangle$ associated with an extended reference molecule as

$$|\phi_i\rangle = \sum_\mu C_{\mu i}|\psi_\mu^{gp}\rangle \tag{6}$$

Specifically, for the alkane junctions considered here, we use the reference system shown in the right panel of Figure 1a, an alkane fragment with three additional Au atoms. Figure 2 (bottom) shows the $|C_{\mu i}|^2$ components and the contributions of the states of the extended molecule in the junction that are closest to the resonance peak at −1.2 eV. The gas-phase orbitals with the largest contribution are also shown in Figure 2. The resonance state exhibits large contributions from the $|\psi_{H-2}^{gp}\rangle$, $|\psi_L^{gp}\rangle$, and $|\psi_{L+1}^{gp}\rangle$ states of our extended gas-phase reference, which now includes Au orbitals.

Figure 3a shows the energy levels associated with the C7+Au$_3$ gas-phase reference; DFT energies at the PBE level are shown in black. Because of the presence of frontier states that are relatively localized on the Au atoms, the PBE HOMO−LUMO (HOMO: highest occupied molecular orbital; LUMO: lowest unoccupied molecular orbital) gap of C7+Au$_3$ is quite small, ∼0.6 eV. Both OT-RSH and *GW* open up this gap to around 5.7 and 5.9 eV, respectively. Notably, the OT-RSH and the *GW* corrections are quite similar for this reference system.

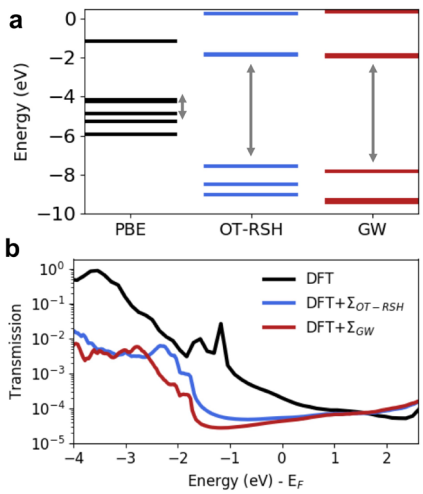

Figure 3. (a) Gas-phase energy levels of the bare C7+Au$_3$ molecule, calculated using PBE (black), OT-RSH (blue), and GW@OT-RSH (red). HOMO−LUMO gaps are shown in gray arrows. (b) Transmission as a function of energy relative to E_F, for the C7 molecular junction, calculated using a generalized Σ shift in eq 7, with the gas-phase correction calculated using OT-RSH (blue) and GW (red) for the C7+Au$_3$ reference and compared with the DFT-PBE transmission (black).

The fact that there are significant contributions from multiple gas-phase states to important resonances in the DFT transmission requires that we consider orbital mixing when applying the gas-phase correction term in DFT+Σ. From eq 3, the diagonal elements in the self-energy correction to the junction Hamiltonian are $\delta H_{ii} = \langle\phi_i|\delta H|\phi_i\rangle = \sum_\mu |C_{\mu i}|^2\Sigma_\mu$. Following the same strategy as eq 5, one should replace Σ_μ by $\Delta_\mu + P_\mu$ for each gas-phase reference orbital. However, another complication arises. As noted, partitioning Σ_μ into Δ_μ and P_μ for a specific gas-phase reference orbital is only exact for near-unity projections. In the C7 junction, the expansion coefficients $C_{\mu i}$ are non-negligible for multiple orbitals, and crucially, the coefficients $C_{\mu i}$ for an occupied (unoccupied) junction orbital ϕ_i do not only involve the occupied (unoccupied) manifold of gas-phase reference orbitals $\{\psi_\mu^{gp}\}$. In other words, occupied and unoccupied orbitals of the gas-phase reference mix with one another in the junction. Physically, this implies nontrivial charge rearrangement between the molecule and the leads, contradicting a primary assumption of the original DFT+Σ framework.

To generalize the self-energy δH for this case, we propose the following approach. We write the corrections δH to the junction orbitals as a weighted average of the gas-phase corrections plus a polarization term, namely

$$\delta H_{ii} \approx \langle\phi_i|\delta H|\phi_i\rangle = \alpha_i \sum_\mu |C_{\mu i}|^2|\Delta_\mu| + P_i \tag{7}$$

In eq 7 we introduce the integer α, which is set by the occupation of the junction orbital ϕ_i; α takes values of −1 for occupied and +1 for unoccupied orbitals. We use the magnitude of the gas-phase correction for a given orbital of the extended molecule, applying a negative or positive sign

DOI: 10.1021/acs.jpcc.8b12124
J. Phys. Chem. C XXXX, XXX, XXX−XXX

depending on whether the junction state ϕ_i is occupied or unoccupied. We note that eq 7 assumes by construction that the junction orbitals are not fractionally occupied, as is the case for the systems considered in this work. If fractionally occupied states indeed appear in the junction subsystem Hamiltonian, then eq 7 becomes ill-defined; this indicates that the choice of extended reference system is inappropriate or that the extension of DFT+Σ we introduce here is not applicable.

This pragmatic approach can be viewed as the simplest approximation consistent with the framework of eq 2, where we restrict our application of the self-energy to a tractable reference subspace. We note that this generalization reduces to the original DFT+Σ approach for cases without mixing of occupied and unoccupied orbitals of the gas-phase reference. We assume that in the more general case of interest here the magnitude of the self-energy corrections to gas-phase orbitals are unchanged by the junction environment; introducing α ensures that the correction has a sign consistent with the occupation of ϕ_i. With minimal additional computational cost, this scheme generalizes the DFT+Σ approach to situations for which there is hybridization between occupied and unoccupied gas-phase orbitals in the junction, such as the case here.

Note that the number of occupied junction orbitals is not necessarily the same as the number of occupied gas-phase reference orbitals due to coupling of the reference subspace to the semi-infinite electrodes. Additionally, P_i is positive (negative) for an occupied (unoccupied) junction orbital. For the choice of a C7+Au_3 gas-phase reference in the C7 junction, the PBE eigenvalues of $|\psi_L^{gp}\rangle$ and $|\psi_{L+1}^{gp}\rangle$ are very close to those of $|\psi_H^{gp}\rangle$ (see Figure 3a); these gas-phase states contribute significantly to occupied ϕ_i in the junction. Accordingly, in those cases, we express Σ for the junction orbitals in terms of the gas-phase orbitals as in eq 7, with $\alpha_i = -1$ and a positive P_i. While this approximation may lead to quantitative differences from a more rigorous *GW* calculation of the junction, it is computationally far less expensive, it is well-defined, orbital-specific, and does not have any free parameters, and it leads to a significant improvement in level alignment over standard DFT for the challenging case of strongly coupled junctions, as we show below.

We further note that we neglect off-diagonal δH_{ij} contributions in eq 3 given the ambiguity in assigning signs for the off-diagonal elements and the fact that the diagonal elements (in the basis of junction orbitals) dominate the transport properties. For simplicity, in what follows, we further use a single P value determined from an image-charge model (but with different signs, as defined above) for all junction orbitals, a simplification consistent with prior work. This approximation can be lifted, in principle, but is, in practice, adequate for the systems studied in this work. Specifically, when Au-localized states are considered, the strong hybridization leads to a spuriously large image-charge correction. Here we avoid this problem by considering just the image-charge corrections of states that are well projected onto junction states, with $|C|^2$ as close to unity as possible. For C7, we hence calculate the image-charge correction based on the well-projected $|\psi_{H-2}^{gp}\rangle$ gas-phase orbital, giving P_{H-2} = 1.6 eV. We use this value as the image-charge correction for all states.

The resulting generalized DFT+Σ transmission is shown as a red line in Figure 3b. The calculated conductance at E_F is 5.3×10^{-5} G_0 for DFT+Σ based on gas-phase OT-RSH corrections and 4.2×10^{-5} G_0 based on gas-phase *GW* corrections; both variants are a considerable improvement in agreement over the DFT-PBE value of 1.9×10^{-4} G_0, with the experimental result of 2.0×10^{-5} G_0.[64] Repeating this analysis for C3 and C5 junctions with a generalized DFT+Σ with gas-phase corrections from OT-RSH (see the SI for details) leads to similarly good agreement with experiment in all cases, as detailed in Table 1.

Table 1. Calculated Conductance (in the unit of G_0) for the Examined Systems Using DFT and DFT+Σ with Gas-Phase Shifts Based on OT-RSH and *GW* for the Reference System of the Alkane Chain and a Au Trimer and Compared with Experiment[64]

	DFT	DFT+Σ	exp.
C3	4.5×10^{-3}	1.0×10^{-3} (OTRSH)	1.0×10^{-3}
C5	1.2×10^{-3}	2.9×10^{-4} (OTRSH)	1.9×10^{-4}
C7	1.9×10^{-4}	5.3×10^{-5} (OTRSH)	2.0×10^{-5}
		4.2×10^{-5} (GW)	

Our generalized DFT+Σ approach suggests that the inclusion of a few lead atoms in our reference can, for covalent systems, lead to accurate corrections to DFT level alignment and predicted conductance values in good agreement with experiment. The choice of reference is system-dependent, and for certain systems, more than one reference might be suitable. For example, for BP junctions (Figure 1b), one could imagine at least two different choices for an extended molecule (Figure 1b, right panels). Thus a natural question centers on how to choose the best reference. Here we suggest two criteria: (i) The best reference should use a minimal number of motif Au atoms to maintain the validity of the image charge approximation and (ii) the best reference orbitals should have near-unity projections with junction orbitals. To illustrate the latter criterion, we examine the well studied BP junction (Figure 1b). This weakly coupled junction's primary transmission peak is known to have LUMO character of the gas-phase molecule.[60,84] Previous works have shown that the bare BP molecule is a good reference system for approximate Σ corrections, and applying the standard DFT+Σ method led to calculated conductances in quantitative agreement with experimental measurements.[60,84] Here we use the "low-conductance" configuration of the BP junction as an example (adopting the junction geometry from previous work[84]) and apply DFT+Σ calculations using two different gas-phase references: the bare molecule, and the molecule with one Au atom from each lead. Following our criteria, we show that the bare BP molecule (with no additional lead atoms) is the better reference system, as we elaborate on below.

Figure 4a (top) shows the calculated DFT transmission curve for a BP junction. The resonance with a peak around 0.3 eV above E_F dominates the conductance through the junction. The eigenchannel associated with this resonance state is also presented. The middle panel of Figure 4a shows the projections $|C_{\mu i}|^2$ of eq 6 for the standard BP molecule gas-phase reference used in prior works. The bottom panel shows these projections for the case of a reference system that includes the bare BP molecule and one Au atom from each lead, namely, Au_1−BP−Au_1. The resonance state in the junction projects fully onto a single orbital, the LUMO, of the bare molecule in the gas phase. For the Au-containing reference system, the situation is more complicated; the resonance state has a significant projection coefficient from a state that is associated with the additional Au atoms as well as

DOI: 10.1021/acs.jpcc.8b12124
J. Phys. Chem. C XXXX, XXX, XXX−XXX

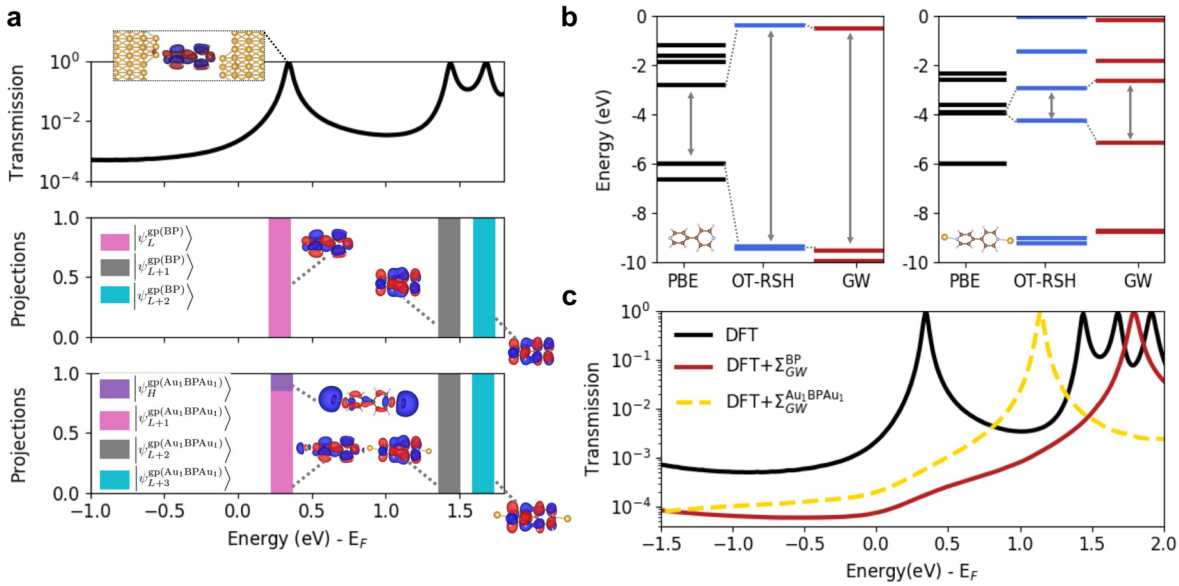

Figure 4. (a) Top: DFT-based transmission as a function of energy relative to E_F for the BP molecular junction. Bottom: Projection coefficients $|C|^2$ of the resonance LUMO state and other unoccupied levels in the case of BP (upper) and Au_1−BP−Au_1 reference systems within the generalized DFT+Σ approach. Each color represents a different gas-phase orbital, shown in the figure. (b) Gas-phase energy levels of the bare BP molecule (left) and the extended Au_1−BP−Au_1 system, calculated using PBE (black lines), OT-RSH (blue lines), and *GW*@OT-RSH (red lines). HOMO−LUMO gaps are shown in gray arrows. (c) Transmission as a function of energy relative to E_F, for the BP molecular junction, calculated using a generalized Σ shift in eq 7, with the gas-phase correction calculated using *GW* for both the bare BP (solid red line) and the extended Au_1−BP−Au_1 (dashed yellow line) molecular references and compared with the DFT-based transmission (black line).

other states. This mixing challenges the use of the extended reference system for BP, and the strong projection onto the bare molecule LUMO favors the bare molecule as a reference in this case. For additional emphasis, Figure 4b shows the energy levels associated with both the bare BP and the Au_1−BP−Au_1 gas-phase references. DFT levels at the PBE level are shown in black; the PBE HOMO−LUMO gap of BP is ∼2.5 eV for BP, and both OT-RSH and *GW* open up this gap to ∼9 eV. For Au_1−BP−Au_1, however, the PBE gap is zero; the HOMO and the LUMO states are practically degenerate in energy. This is because these states are highly localized on the Au atoms. (See Figure S1, in which we compare the energy levels and wave functions associated with three different BP reference systems: the bare molecule, Au_1−BP−Au_1, and Au_3−BP−Au_3.) Introducing OT-RSH or *GW* corrections opens up the gap, however, not to the extent of the BP gap. We note that unlike in the alkane chain junctions presented above, in this case, the OT-RSH corrections are different than the *GW* ones. The OT-RSH parameter tuning is more challenging for this system because of the presence of both highly localized and delocalized states.[85] In addition, the one-shot G_0W_0 we use may also carry an error due to the starting point and the lack of self-consistency, as discussed above. The highly Au-localized states also challenge our image-charge correction model for nonlocal polarization effects, as discussed above. However, as for the case of C7+Au_3, we can use a well-projected orbital to set a common *P* for all states: For the bare BP, the gas-phase $|\psi_L^{gp}\rangle$ is well projected, as shown in Figure 4a, resulting in P_{LUMO}^{BP} = 0.8 eV. For the Au_1−BP−Au_1 reference, the gas-phase $|\psi_{L+1}^{gp}\rangle$ is well projected onto the resonance state, resulting in P_{LUMO}^{BP} = 0.9 eV.

When used with eq 7, the calculated energy level shifts give rise to the transmission shown in Figure 4c. The OT-RSH- and *GW*-based Σ corrections for the bare BP reference system result in very similar conductance values of 0.6×10^{-4} G_0 and 0.7×10^{-4} G_0, respectively, which compare well with the experimental result of 1.6×10^{-4} G_0.[84] (We show only the *GW*-based DFT+Σ transmission for brevity; see the SI for the OT-RSH-based results.) For the Au_1−BP−Au_1 reference system, the resulting transmissions are fairly similar (because the junction states dominating the transmission do not include localized Au orbitals), but the resonance state is noticeably shifted to lower energies, resulting from the fact that no single Au_1−BP−Au_1 orbital perfectly projects onto any junction state and most likely also from challenges associated with calculations of the energy levels for the gas-phase reference in this case. The Au_1−BP−Au_1 reference system leads to a conductance value of 2.0×10^{-4} G_0, a result close to the experimental value (which is an average value over many junction geometries). However, guided by the molecular orbital projections and based on the reasoning above, we consider the bare molecule to be a more justified reference that leads to a more accurate transmission function for this particular junction geometry, and we recommend the bare molecule as a reference for this case.

Our results provide a means by which the DFT+Σ framework can be generalized to a broad range of molecular junctions, including those with covalent binding, through the use of an extended reference system that includes lead atoms. We note, however, that when including Au atoms in the gas-phase reference system, special care should be taken because some of the gas-phase states are highly localized on metallic states that are not associated with conducting orbitals of the junction, and a one-to-one correspondence between molecular and junction orbitals is not guaranteed. Our suggested generalized DFT+Σ framework, eq 7, resolves this issue by introducing a self-energy correction based on the mixing of gas-phase orbitals upon the formation of the junction. The reference system is chosen to be charge-neutral and closed-shell, but it is not unique. A judicious choice involves the

DOI: 10.1021/acs.jpcc.8b12124
J. Phys. Chem. C XXXX, XXX, XXX−XXX

atoms participating in the covalent binding and the minimal number of lead atoms necessary for a gas-phase orbital to resemble the junction conducting orbital; we also select our reference so as to obtain orbitals that are closest to having near-unity projections on the junction orbitals. As shown above, for the examined covalent junctions, this approach can account for important molecule-lead hybridization effects and lead to considerable quantitative improvement over DFT conductance values at a computational cost far less than a full *GW* calculation of the junction.

In general, we note that we do not expect that adding more lead atoms to the reference system will necessarily give rise to better results within the DFT+Σ formalism. In eq 3, we introduce a self-energy correction to the reference subsystem in the junction, correcting the eigenvalues of this subblock of the Hamiltonian. This ansatz implicitly assumes that the orbitals of the reference (eigenvectors of this subblock of junction Hamiltonian) do not change significantly when the reference subsystem is attached to the other parts of the scattering region. With more lead atoms included in the reference system, this assumption may break down, and it is no longer clear how the self-energy correction should be defined. Additionally, as the number of lead atoms increases, the approximate approach used here to capture "image charge effects" (e.g., renormalization of molecular states/energies by the leads), embodied in the image charge (or nonlocal polarization) term of eq 5, will become increasingly irrelevant and redundant as the number of lead atoms in the reference grows. These arguments, and the validation from the results of our calculations on the systems studied here, motivate the ansatz that one should use a minimal number of lead atoms here, leading to the best projection of the reference orbitals onto the junction eigenchannel. As we show here, including a minimal number of lead atoms that correctly reflects the hybridization between the molecule and the electrode greatly improves the quantitative agreement with experiment in the systems examined in this work.

In Figure 5, we summarize with our recipe generalizing the DFT+Σ approach for strongly and covalently bound molecular junctions. First, a transmission calculation based on local or semilocal functionals is performed, and the resonance state dominating the conductance is identified. A suitable reference system is then defined (including the molecule and a minimal number lead atoms at the contact motif), for which there should be an orbital in the gas phase that strongly projects (as near unity as possible) onto the junction state that determines conductance. We require that the reference system is charge-neutral and closed-shell. The projections of the junction orbital (eigenstates of the reference subblock in junction Hamiltonian) onto the gas-phase reference orbitals are calculated using eq 6, and the self-energy correction is calculated using eq 7, with orbital-specific gas-phase shifts weighted by the expansion coefficients. The renormalization of molecular energies due to nonlocal polarization by the leads can be computed, for example, with an image-charge correction calculated following, for example, ref 69, for the state that is well-projected onto the resonance eigenchannels.

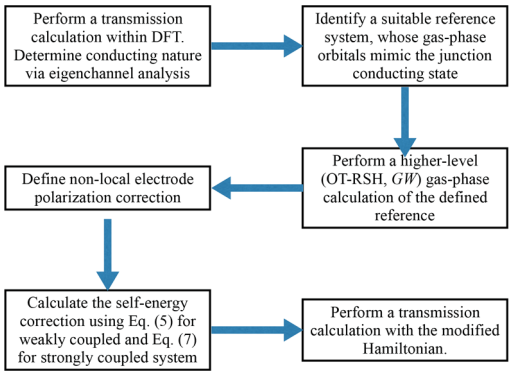

Figure 5. Summary of the workflow of the DFT+Σ approach.

CONCLUSIONS

We have presented an approach to accurately calculate transport properties through covalently bound molecular junctions, a generalization of the DFT+Σ method. In particular, we propose criteria to select an extended gas-phase reference system, which can include a few lead atoms, and evaluate an approximate Σ correction based on this reference system. We also propose an approach to the gas-phase correction that takes into account the hybridization of gas-phase reference orbitals upon the formation of the junction. We demonstrated our approach using junctions with covalent carboxylic binding and revisited the weakly coupled Au−BP−Au junction with new insights and discussed related subtleties. We have demonstrated that this method is able to predict conductance on par with experimental results, fully from first-principles with no empirical parameters, at relatively low computational cost and therefore will be of use for interpreting the transport properties of broad classes of molecular junctions.

ASSOCIATED CONTENT

Supporting Information

The Supporting Information is available free of charge on the ACS Publications website at DOI: 10.1021/acs.jpcc.8b12124.

Full computational details and additional data on BP transmission and gas-phase orbitals (PDF)

AUTHOR INFORMATION

Corresponding Author

*E-mail: jbneaton@lbl.gov.

ORCID

Sivan Refaely-Abramson: 0000-0002-7031-8327

Zhen-Fei Liu: 0000-0002-2423-8430

Notes

The authors declare no competing financial interest.

ACKNOWLEDGMENTS

This work was supported by the U.S. Department of Energy, Office of Basic Energy Sciences, Materials Sciences and Engineering Division under contract no. DE-AC02-05CH11231 within the Theory FWP. This work was also supported with computational resources by the Molecular Foundry through the U.S. Department of Energy, Office of Basic Energy Sciences under the same contract number. Portions of the computational work were performed at the National Energy Research Scientific Computing Center. S.R.-A. acknowledges Fulbright and Rothschild Fellowships. F.B. acknowledges high-performance computing resources from GENCI-CCRT-TGCC (Grants No. 2017-096018).

REFERENCES

(1) Nitzan, A.; Ratner, M. A. Electron Transport in Molecular Wire Junctions. *Science* **2003**, *300*, 1384−1389.

(2) Tao, N. J. Electron Transport in Molecular Junctions. *Nat. Nanotechnol.* **2006**, *1*, 173−181.

(3) Aradhya, S. V.; Venkataraman, L. Single-Molecule Junctions Beyond Electronic Transport. *Nat. Nanotechnol.* **2013**, *8*, 399−410.

(4) Schwarz, F.; Loertscher, E. Break-Junctions for Investigating Transport at the Molecular Scale. *J. Phys.: Condens. Matter* **2014**, *26*, 474201.

(5) Thompson, D.; Nijhuis, C. A. Even the Odd Numbers Help: Failure Modes of SAM-Based Tunnel Junctions Probed via Odd-Even Effects Revealed in Synchrotrons and Supercomputers. *Acc. Chem. Res.* **2016**, *49*, 2061−2069.

(6) Xiang, D.; Wang, X.; Jia, C.; Lee, T.; Guo, X. Molecular-Scale Electronics: From Concept to Function. *Chem. Rev.* **2016**, *116*, 4318−4440.

(7) Wang, K.; Xu, B. Modulation and Control of Charge Transport Through Single-Molecule Junctions. *Top. Curr. Chem.* **2017**, *375*, 17.

(8) Quek, S. Y.; Khoo, K. H. Predictive DFT-Based Approaches to Charge and Spin Transport in Single-Molecule Junctions and Two-Dimensional Materials: Successes and Challenges. *Acc. Chem. Res.* **2014**, *47*, 3250−3257.

(9) Perroni, C. A.; Ninno, D.; Cataudella, V. Thermoelectric Efficiency of Molecular Junctions. *J. Phys.: Condens. Matter* **2016**, *28*, 373001.

(10) Thoss, M.; Evers, F. Theory of Quantum Transport in Molecular Junctions. *J. Chem. Phys.* **2018**, *148*, 030901.

(11) Huang, C.; Rudnev, A. V.; Hong, W.; Wandlowski, T. Break Junction Under Electrochemical Gating: Testbed for Single-Molecule Electronics. *Chem. Soc. Rev.* **2015**, *44*, 889−901.

(12) Perrin, M. L.; Burzuri, E.; van der Zant, H. S. J. Single-Molecule Transistors. *Chem. Soc. Rev.* **2015**, *44*, 902−919.

(13) Vilan, A.; Aswal, D.; Cahen, D. Large-Area, Ensemble Molecular Electronics: Motivation and Challenges. *Chem. Rev.* **2017**, *117*, 4248−4286.

(14) Capozzi, B.; Xia, J.; Adak, O.; Dell, E. J.; Liu, Z.-F.; Taylor, J. C.; Neaton, J. B.; Campos, L. M.; Venkataraman, L. Single-Molecule Diodes with High Rectification Ratios Through Environmental Control. *Nat. Nanotechnol.* **2015**, *10*, 522−527.

(15) Nichols, R. J.; Higgins, S. J. Single Molecule Nano-electrochemistry in Electrical Junctions. *Acc. Chem. Res.* **2016**, *49*, 2640−2648.

(16) Jia, C.; Guo, X. Molecule-Electrode Interfaces in Molecular Electronic Devices. *Chem. Soc. Rev.* **2013**, *42*, 5642−5660.

(17) Leary, E.; La Rosa, A.; Gonzalez, M. T.; Rubio-Bollinger, G.; Agrait, N.; Martin, N. Incorporating Single Molecules into Electrical Circuits. The Role of The Chemical Anchoring Group. *Chem. Soc. Rev.* **2015**, *44*, 920−942.

(18) Su, T. A.; Neupane, M.; Steigerwald, M. L.; Venkataraman, L.; Nuckolls, C. Chemical Principles of Single-Molecule Electronics. *Nat. Rev. Mater.* **2016**, *1*, 16002.

(19) Su, T. A.; Li, H.; Klausen, R. S.; Kim, N. T.; Neupane, M.; Leighton, J. L.; Steigerwald, M. L.; Venkataraman, L.; Nuckolls, C. Silane and Germane Molecular Electronics. *Acc. Chem. Res.* **2017**, *50*, 1088−1095.

(20) Paulsson, M.; Frederiksen, T.; Brandbyge, M. Molecular Electronics: Insight from First-Principles Transport Simulations. *Chimia* **2010**, *64*, 350−355.

(21) Nakamura, H..*Single-Molecule Electronics*; Kiguchi, K., Ed.; Springer: Singapore, 2016.

(22) Saraiva-Souza, A.; Smeu, M.; Zhang, L.; Souza Filho, A. G.; Guo, H.; Ratner, M. A. Molecular Spintronics: Destructive Quantum Interference Controlled by a Gate. *J. Am. Chem. Soc.* **2014**, *136*, 15065−15071.

(23) Xu, B.; Dubi, Y. Negative Differential Conductance in Molecular Junctions: an Overview of Experiment and Theory. *J. Phys.: Condens. Matter* **2015**, *27*, 263202.

(24) Liu, Z.; Ren, S.; Guo, X. Switching Effects in Molecular Electronic Devices. *Top. Curr. Chem.* **2017**, *375*, 56.

(25) Liu, Z.-F.; Neaton, J. B. Voltage Dependence of Molecule-Electrode Coupling in Biased Molecular Junctions. *J. Phys. Chem. C* **2017**, *121*, 21136−21144.

(26) Mowbray, D. J.; Jones, G.; Thygesen, K. S. Influence of Functional Groups on Charge Transport in Molecular Junctions. *J. Chem. Phys.* **2008**, *128*, 111103.

(27) Jia, C.; Ma, B.; Xin, N.; Guo, X. Carbon Electrode-Molecule Junctions: A Reliable Platform for Molecular Electronics. *Acc. Chem. Res.* **2015**, *48*, 2565−2575.

(28) Li, Z.; Smeu, M.; Rives, A.; Maraval, V.; Chauvin, R.; Ratner, M. A.; Borguet, E. Towards Graphyne Molecular Electronics. *Nat. Commun.* **2015**, *6*, 6321.

(29) Van Dyck, C.; Ratner, M. A. Molecular Rectifiers: A New Design Based on Asymmetric Anchoring Moieties. *Nano Lett.* **2015**, *15*, 1577−1584.

(30) Baldea, I. Transition Voltage Spectroscopy Reveals Significant Solvent Effects on Molecular Transport and Settles an Important Issue in Bipyridine-Based Junctions. *Nanoscale* **2013**, *5*, 9222−9230.

(31) Kotiuga, M.; Darancet, P.; Arroyo, C. R.; Venkataraman, L.; Neaton, J. B. Adsorption-Induced Solvent-Based Electrostatic Gating of Charge Transport through Molecular Junctions. *Nano Lett.* **2015**, *15*, 4498−4503.

(32) Cheung, K. C. M.; Chen, X.; Albrecht, T.; Kornyshev, A. A. Principles of a Single-Molecule Rectifier in Electrolytic Environment. *J. Phys. Chem. C* **2016**, *120*, 3089−3106.

(33) Li, X.; Hu, D.; Tan, Z.; Bai, J.; Xiao, Z.; Yang, Y.; Shi, J.; Hong, W. Supramolecular Systems and Chemical Reactions in Single-Molecule Break Junctions. *Top. Curr. Chem.* **2017**, *375*, 42.

(34) Aragonés, A. C.; Haworth, N. L.; Darwish, N.; Ciampi, S.; Bloomfield, N. J.; Wallace, G. G.; Diez-Perez, I.; Coote, M. L. Electrostatic Catalysis of a Diels-Alder Reaction. *Nature* **2016**, *531*, 88−91.

(35) Schubert, C.; Margraf, J. T.; Clark, T.; Guldi, D. M. Molecular Wires - Impact of Pi-Conjugation and Implementation of Molecular Bottlenecks. *Chem. Soc. Rev.* **2015**, *44*, 988−998.

(36) Zimbovskaya, N. A. Seebeck Effect in Molecular Junctions. *J. Phys.: Condens. Matter* **2016**, *28*, 183002.

(37) Meir, Y.; Wingreen, N. S. Landauer Formula for the Current Through an Interacting Electron Region. *Phys. Rev. Lett.* **1992**, *68*, 2512−2515.

(38) Haug, H. J. W.; Jauho, A.-P. *Quantum Kinetics in Transport and Optics of Semiconductors*, 2nd ed.; Springer: Berlin, 2007.

(39) Taylor, J.; Guo, H.; Wang, J. *Ab Initio* Modeling of Quantum Transport Properties of Molecular Electronic Devices. *Phys. Rev. B: Condens. Matter Mater. Phys.* **2001**, *63*, 245407.

(40) Brandbyge, M.; Mozos, J.-L.; Ordejón, P.; Taylor, J.; Stokbro, K. Density-Functional Method for Nonequilibrium Electron Transport. *Phys. Rev. B: Condens. Matter Mater. Phys.* **2002**, *65*, 165401.

(41) Thygesen, K.; Jacobsen, K. Molecular Transport Calculations with Wannier Functions. *Chem. Phys.* **2005**, *319*, 111−125.

(42) Perdew, J. P.; Parr, R. G.; Levy, M.; Balduz, J. L. Density-Functional Theory for Fractional Particle Number: Derivative Discontinuities of the Energy. *Phys. Rev. Lett.* **1982**, *49*, 1691−1694.

(43) Perdew, J. P.; Levy, M. Physical Content of the Exact Kohn-Sham Orbital Energies: Band Gaps and Derivative Discontinuities. *Phys. Rev. Lett.* **1983**, *51*, 1884−1887.

(44) Sham, L. J.; Schlüter, M. Density-Functional Theory of the Energy Gap. *Phys. Rev. Lett.* **1983**, *51*, 1888−1891.

(45) Kümmel, S.; Kronik, L. Orbital-Dependent Density Functionals: Theory and Applications. *Rev. Mod. Phys.* **2008**, *80*, 3−60.

(46) Kronik, L.; Stein, T.; Refaely-Abramson, S.; Baer, R. Excitation Gaps of Finite-Sized Systems from Optimally Tuned Range-Separated Hybrid Functionals. *J. Chem. Theory Comput.* **2012**, *8*, 1515−1531.

(47) Neaton, J. B.; Hybertsen, M. S.; Louie, S. G. Renormalization of Molecular Electronic Levels at Metal-Molecule Interfaces. *Phys. Rev. Lett.* **2006**, *97*, 216405.

DOI: 10.1021/acs.jpcc.8b12124
J. Phys. Chem. C XXXX, XXX, XXX−XXX

(48) Dell'Angela, M.; Kladnik, G.; Cossaro, A.; Verdini, A.; Kamenetska, M.; Tamblyn, I.; Quek, S. Y.; Neaton, J. B.; Cvetko, D.; Morgante, A.; et al. Relating Energy Level Alignment and Amine-Linked Single Molecule Junction Conductance. *Nano Lett.* **2010**, *10*, 2470−2474.
(49) Quek, S. Y.; Venkataraman, L.; Choi, H. J.; Louie, S. G.; Hybertsen, M. S.; Neaton, J. B. Amine Gold Linked Single-Molecule Circuits: Experiment and Theory. *Nano Lett.* **2007**, *7*, 3477−3482.
(50) Hedin, L. New Method for Calculating the One-Particle Green's Function with Application to the Electron-Gas Problem. *Phys. Rev.* **1965**, *139*, A796−A823.
(51) Hybertsen, M. S.; Louie, S. G. First-Principles Theory of Quasiparticles: Calculation of Band Gaps in Semiconductors and Insulators. *Phys. Rev. Lett.* **1985**, *55*, 1418−1421.
(52) Hybertsen, M. S.; Louie, S. G. Electron Correlation in Semiconductors and Insulators: Band Gaps and Quasiparticle Energies. *Phys. Rev. B: Condens. Matter Mater. Phys.* **1986**, *34*, 5390−5413.
(53) Thygesen, K. S.; Rubio, A. Conserving *GW* Scheme for Nonequilibrium Quantum Transport in Molecular Contacts. *Phys. Rev. B: Condens. Matter Mater. Phys.* **2008**, *77*, 115333.
(54) Blase, X.; Attaccalite, C.; Olevano, V. First-Principles *GW* Calculations for Fullerenes, Porphyrins, Phtalocyanine, and Other Molecules of Interest for Organic Photovoltaic Applications. *Phys. Rev. B: Condens. Matter Mater. Phys.* **2011**, *83*, 115103.
(55) Bruneval, F.; Marques, M. A. L. Benchmarking the Starting Points of the GW Approximation for Molecules. *J. Chem. Theory Comput.* **2013**, *9*, 324−329.
(56) Wilhelm, J.; Del Ben, M.; Hutter, J. *GW* in the Gaussian and Plane Waves Scheme with Application to Linear Acenes. *J. Chem. Theory Comput.* **2016**, *12*, 3623−3635.
(57) Pauly, F.; Viljas, J. K.; Huniar, U.; Häfner, M.; Wohlthat, S.; Bürkle, M.; Cuevas, J. C.; Schön, G. Cluster-Based Density-Functional Approach to Quantum Transport Through Molecular and Atomic Contacts. *New J. Phys.* **2008**, *10*, 125019.
(58) Rangel, T.; Ferretti, A.; Trevisanutto, P. E.; Olevano, V.; Rignanese, G.-M. Transport Properties of Molecular Junctions from Many-Body Perturbation Theory. *Phys. Rev. B: Condens. Matter Mater. Phys.* **2011**, *84*, 045426.
(59) Ryndyk, D. A.; Donarini, A.; Grifoni, M.; Richter, K. Many-Body Localized Molecular Orbital Approach to Molecular Transport. *Phys. Rev. B: Condens. Matter Mater. Phys.* **2013**, *88*, 085404.
(60) Quek, S. Y.; Kamenetska, M.; Steigerwald, M. L.; Choi, H. J.; Louie, S. G.; Hybertsen, M. S.; Neaton, J. B.; Venkataraman, L. Mechanically Controlled Binary Conductance Switching of a Single-Molecule Junction. *Nat. Nanotechnol.* **2009**, *4*, 230−234.
(61) Widawsky, J. R.; Darancet, P.; Neaton, J. B.; Venkataraman, L. Simultaneous Determination of Conductance and Thermopower of Single Molecule Junctions. *Nano Lett.* **2012**, *12*, 354−358.
(62) Darancet, P. T.; Widawsky, J. R.; Choi, H. J.; Venkataraman, L.; Neaton, J. B. Quantitative Current-Voltage Characteristics in Molecular Junctions from First Principles. *Nano Lett.* **2012**, *12*, 6250−6254.
(63) Liu, Z.-F.; Wei, S.; Yoon, H.; Adak, O.; Ponce, I.; Jiang, Y.; Jang, W.-D.; Campos, L. M.; Venkataraman; Neaton, J. B. Control of Single-Molecule Junction Conductance of Porphyrins via a Transition-Metal Center. *Nano Lett.* **2014**, *14*, 5365−5370.
(64) Brisendine, J. M.; Refaely-Abramson, S.; Liu, Z.-F.; Cui, J.; Ng, F.; Neaton, J. B.; Koder, R. L.; Venkataraman, L. Probing Charge Transport through Peptide Bonds. *J. Phys. Chem. Lett.* **2018**, *9*, 763−767.
(65) Chen, W.; Widawsky, J. R.; Vázquez, H.; Schneebeli, S. T.; Hybertsen, M. S.; Breslow, R.; Venkataraman, L. Highly Conducting π-Conjugated Molecular Junctions Covalently Bonded to Gold Electrodes. *J. Am. Chem. Soc.* **2011**, *133*, 17160−17163.
(66) Strange, M.; Rostgaard, C.; H akkinen, M.; Thygesen, K. S. Self-Consistent GW Calculations of Electronic Transport in Thiol-and Amine-Linked Molecular Junctions. *Phys. Rev. B: Condens. Matter Mater. Phys.* **2011**, *83*, 115108.
(67) Rangel, T.; Ferretti, A.; Olevano, V.; Rignanese, G.-M. Many-Body Correlations and Coupling in Benzene-Dithiol Junctions. *Phys. Rev. B: Condens. Matter Mater. Phys.* **2017**, *95*, 115137.
(68) Brandbyge, M.; Mozos, J.-L.; Ordejón, P.; Taylor, J.; Stokbro, K. Density-Functional Method for Nonequilibrium Electron Transport. *Phys. Rev. B: Condens. Matter Mater. Phys.* **2002**, *65*, 165401.
(69) Egger, D. A.; Liu, Z.-F.; Neaton, J. B.; Kronik, L. Reliable Energy Level Alignment at Physisorbed MoleculeMetal Interfaces from Density Functional Theory. *Nano Lett.* **2015**, *15*, 2448−2455.
(70) Soler, J. M.; Artacho, E.; Gale, J. D.; García, A.; Junquera, J.; Ordejón, P.; Sánchez-Portal, D. The SIESTA Method for Ab Initio Order-N Materials Simulation. *J. Phys.: Condens. Matter* **2002**, *14*, 2745−2779.
(71) Nitzan, A. *Chemical Dynamics in Condensed Phases: Relaxation, Transfer and Reactions in Condensed Molecular Systems*; Oxford University Press, 2006.
(72) Perdew, J. P.; Burke, K.; Ernzerhof, M. Generalized Gradient Approximation Made Simple. *Phys. Rev. Lett.* **1996**, *77*, 3865−3868.
(73) Shao, Y.; Molnar, L. F.; Jung, Y.; Kussmann, J.; Ochsenfeld, C.; Brown, S. T.; Gilbert, A. T. B.; ila, V.; Slipchenko, L.; Levchenko, S. V.; et al. Advances in Methods and Algorithms in a Modern Quantum Chemistry Program Package. *Phys. Chem. Chem. Phys.* **2006**, *8*, 3172−3191.
(74) Bruneval, F.; Rangel, T.; Hamed, S. M.; Shao, M.; Yang, C.; Neaton, J. MOLGW 1: Many-Body Perturbation Theory Software for Atoms, Molecules, and Clusters. *Comput. Phys. Commun.* **2016**, *208*, 149−161.
(75) Xu, B.; Tao, N. J. Measurement of Single-Molecule Resistance by Repeated Formation of Molecular Junctions. *Science* **2003**, *301*, 1221−1223.
(76) Salomon, A.; Cahen, D.; Lindsay, S.; Tomfohr, J.; Engelkes, V.; Frisbie, C. Comparison of Electronic Transport Measurements on Organic Molecules. *Adv. Mater.* **2003**, *15*, 1881−1890.
(77) Engelkes, V. B.; Beebe, J. M.; Frisbie, C. D. Length-Dependent Transport in Molecular Junctions Based on SAMs of Alkanethiols and Alkanedithiols:‰ Effect of Metal Work Function and Applied Bias on Tunneling Efficiency and Contact Resistance. *J. Am. Chem. Soc.* **2004**, *126*, 14287−14296.
(78) Venkataraman, L.; Klare, J. E.; Tam, I. W.; Nuckolls, C.; Hybertsen, M. S.; Steigerwald, M. L. Single-Molecule Circuits with Well-Defined Molecular Conductance. *Nano Lett.* **2006**, *6*, 458−462.
(79) Park, Y. S.; Whalley, A. C.; Kamenetska, M.; Steigerwald, M. L.; Hybertsen, M. S.; Nuckolls, C.; Venkataraman, L. Contact Chemistry and Single-Molecule Conductance: A Comparison of Phosphines, Methyl Sulfides, and Amines. *J. Am. Chem. Soc.* **2007**, *129*, 15768−15769.
(80) Paulsson, M.; Krag, C.; Frederiksen, T.; Brandbyge, M. Conductance of Alkanedithiol Single-Molecule Junctions: A Molecular Dynamics Study. *Nano Lett.* **2009**, *9*, 117−121.
(81) Liu, H.; Wang, N.; Zhao, J.; Guo, Y.; Yin, X.; Boey, F. Y. C.; Zhang, H. Length-Dependent Conductance of Molecular Wires and Contact Resistance in Metal-Molecule-Metal Junctions. *ChemPhysChem* **2008**, *9*, 1416−1424.
(82) Ahn, S.; Aradhya, S. V.; Klausen, R. S.; Capozzi, B.; Roy, X.; Steigerwald, M. L.; Nuckolls, C.; Venkataraman, L. Electronic Transport and Mechanical Stability of Carboxyl Linked Single-Molecule Junctions. *Phys. Chem. Chem. Phys.* **2012**, *14*, 13841−13845.
(83) Paulsson, M.; Brandbyge, M. Transmission Eigenchannels from Nonequilibrium Greens Functions. *Phys. Rev. B: Condens. Matter Mater. Phys.* **2007**, *76*, 115117.
(84) Kim, T.; Darancet, P.; Widawsky, J. R.; Kotiuga, M.; Quek, S. Y.; Neaton, J. B.; Venkataraman, L. Determination of Energy Level Alignment and Coupling Strength in 4, 4-Bipyridine Single-Molecule Junctions. *Nano Lett.* **2014**, *14*, 794−798.
(85) Refaely-Abramson, S.; Sharifzadeh, S.; Govind, N.; Autschbach, J.; Neaton, J. B.; Baer, R.; Kronik, L. Quasiparticle Spectra from a Nonempirical Optimally Tuned Range-Separated Hybrid Density Functional. *Phys. Rev. Lett.* **2012**, *109*, 226405.

DOI: 10.1021/acs.jpcc.8b12124
J. Phys. Chem. C XXXX, XXX, XXX−XXX